JOURNAL OF GUIDANCE, CONTROL, AND DYNAMICS
Vol. 18, No. 4, July–August 1995

Optimal Modal-Space Controller for Structural Damping Enhancements

Min-Hung Hsiao*
Taipei Institute of Technology, Taiwan, Republic of China
Jen-Kuang Huang†
Old Dominion University, Norfolk, Virginia 23529-0247
and
Lawrence W. Taylor Jr.‡
NASA Langley Research Center, Hampton, Virginia 23681-0001

A stochastic optimum-based compensator is developed to enhance structural damping with collocated rate sensors/actuators. This controller is based on explicit solutions for the Riccati equations from a modal-space model. The performance of each controlled mode can be easily adjusted by the corresponding design parameters in the controller. NASA's Spacecraft Control Laboratory Experiment facility is used to demonstrate the effectiveness of this control design. A distributed-parameter model is first obtained by using Holzer's transfer matrix method and the corresponding modal parameters are identified. Then the distributed-parameter model is reduced to a finite-dimensional modal-space model for the controller design. Three torque actuators and three collocated rate sensors are used to suppress the vibration of the first five modes. Analytical and experimental results show that the proposed controller is effective in damping enhancements for large flexible structures.

Introduction

CERTAIN future missions in space require levels of structural stability that can be obtained only through active control. Control system design for large flexible structures is a challenging problem because of their special dynamic characteristics, which include a large number of significant elastic modes with very small inherent damping and inaccuracies in the knowledge of the modal parameters. There are two major approaches to controller design: 1) model-based controllers that employ a state estimator based on the knowledge of the plant such as the linear quadratic Gaussian (LQG) method[1] and pole assignment and 2) model-independent controllers that are viewed as a virtual passive damping system.[2,3] In the LQG approach, a large-dimensional Riccati equation needs to be numerically solved for large flexible structures. Recently, an explicit solution to the LQG problem for flexible structures with collocated rate sensors has been found.[4] However, because the design parameters are few, the performance of the controller may be degraded if the desired controlled modes are increased. On the other hand, it is often too difficult to adjust a variety of design parameters so that they satisfy a specific performance requirement for the model-independent controllers. In this paper, the LQG problem is formulated by using a modal coordinate instead of a physical coordinate. Explicit solutions of the corresponding Riccati equations are then derived so that numerical calculations for solving these equations are no longer required. In addition, the number of design parameters in the optimal controller or the optimal estimator is the same as the number of the controlled modes. Each controller design parameter weighs the contribution of actuators to the performance of a specific mode. Similarly, each estimator design parameter weighs the contribution of the sensors to the estimate of a specific modal state. The closed-loop dampings are also attainable from these design parameters. Therefore, it is easier to determine the design parameters, and thus to achieve a good performance, using this proposed explicit LQG controller design.

Received Sept. 15, 1993; revision received Oct. 17, 1994; accepted for publication Nov. 4, 1994.

*Associate Professor, Department of Mechanical Engineering.
†Associate Professor, Department of Mechanical Engineering. Member AIAA.
‡Chief Scientist, Guidance and Control Division.

In system modeling, a satisfactory finite element model for a flexible structure may require a large number of degrees of freedom (>50), so that more effort is needed in solving eigenvalue problems and model reduction for further controller design. Compared with the finite element model, the distributed-parameter model offers the advantage of a comprehensive dynamics description of flexible structures with a minimal number of modal parameters. Thus, it is easier to identify the modal parameters by using the distributed-parameter model than by using the finite element model.[5,6] The main advantage of the finite element method over distributed-parameter modeling is the ease with which computer models can be generated for various structural geometry. Recently, a computer code[7] has been developing to derive distributed-parameter models for relatively complex geometry structures by using Holzer's transfer matrix method.[8–10] Any large flexible structures can be broken down into substructures with simple elastic and dynamic properties. For each single element, such as a beam, a tether, or a rigid body, one can derive the corresponding transfer matrix. The transfer matrix represents the relationship between two ends of each element by taking a Laplace transformation for each dynamic equation and solving each differential equation with respect to spatial coordinate. Combining these element matrices enables the solution of the global system equations.

To illustrate the controller design, NASA's Spacecraft Control Laboratory Experiment (SCOLE) configuration (see Fig. 1) is provided. The SCOLE facility consists of a heavy "Space Shuttle" body to which is attached a reflector by a flexible mast. For the tests of this paper, the Space Shuttle body is fixed. Three reaction wheels and one three-axis rate gyroscope are used as torque actuators and rate sensors. They are mounted on the attached point of the mast and the reflector. From open-loop testing, it is known that the sixth modal excitation will free decay 95% in about 2 s with more than 10 Hz frequency. Therefore, only the first five modes are chosen as the controlled modes. The design challenge arises not only because of its very low damping and plant uncertainties, but also because of the fact that there are only a few actuators available (three actuators are used to control five modes). In this paper, a distributed-parameter model for the SCOLE configuration is first derived by using the transfer matrix method. The distributed-parameter model is then reduced to a finite-dimensional model in modal space and the proposed explicit LQG controller is introduced. Finally, both analytical and experimental results demonstrate that

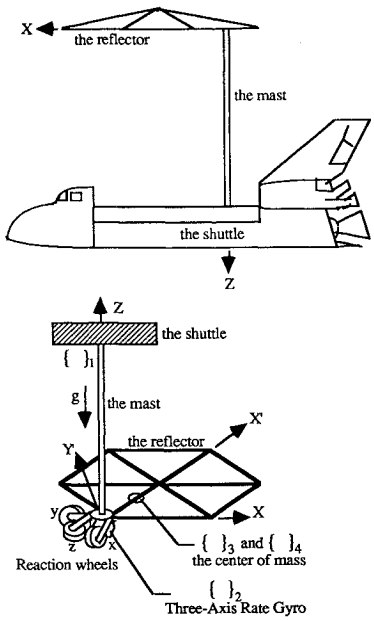

Fig. 1 NASA's SCOLE configuration.

the vibrations can be effectively suppressed by the explicit LQG controller.

Distributed-Parameter Modeling

In this section, the distributed-parameter model of NASA's SCOLE configuration is first derived by using Holzer's transfer matrix method. Then the distributed-parameter model is reduced to a finite-dimensional linear time-invariant model for further control design. A simplified version of the SCOLE model (see Fig. 1) is used to represent a flexible mast clamped at one end (the shuttle end) and an offset reflector attached to the other end of the mast. Thus the mast is modeled by an equivalent uniform Bernoulli beam of length L along the z axis extending from zero, the clamped end, to L, the reflector end. The reflector is treated as a rigid body with small motions. Considering a rigid body subjected to two forces $-f_i$ and f_{i+1} at its center of mass, the side force of gravity f_g, and two torques $-\tau_i$ and τ_{i+1}, the force and the torque balance equations yield

$$m_i \ddot{w}_i = f_{i+1} - f_i + f_g \tag{1}$$

$$J_i \ddot{\theta}_i = \tau_{i+1} - \tau_i \tag{2}$$

where m is the rigid-body mass, w the linear displacement vector, J the moment of inertia matrix of the rigid body, and θ the angular displacement vector. The subscript represents the acting point. Because both ith and $(i+1)$th points are located at the center of mass of the rigid body, we have

$$w_{i+1} = w_i \tag{3}$$

$$\theta_{i+1} = \theta_i \tag{4}$$

For small motions, the side force of gravity is

$$f_g = G_i \theta_i \tag{5}$$

where

$$G_i = \begin{bmatrix} 0 & mg & 0 \\ -mg & 0 & 0 \\ 0 & 0 & 0 \end{bmatrix}$$

After taking a Laplace transformation for the above equations, one can derive

$$\begin{Bmatrix} x \\ q \end{Bmatrix}_{i+1} = \begin{bmatrix} I & 0 \\ s^2\bar{M} + \bar{G} & I \end{bmatrix}_i \begin{Bmatrix} x \\ q \end{Bmatrix}_i \tag{6}$$

where

$$x = \begin{Bmatrix} w \\ \theta \end{Bmatrix}$$

is the displacement vector,

$$q = \begin{Bmatrix} f \\ \tau \end{Bmatrix}$$

the generalized force vector,

$$\bar{M} = \begin{bmatrix} mI & 0 \\ 0 & J \end{bmatrix}, \qquad \bar{G} = \begin{bmatrix} 0 & G \\ 0 & 0 \end{bmatrix}$$

and I an identity matrix. This equation represents the rigid-body dynamics subjected to two force systems located at the center of the mass and the side force of gravity.

Let r_i denote the distance vector $\{r_x, r_y, r_z\}_i^T$ from the ith point to the $(i+1)$th point. Then we can relate the displacement vectors between the ith and the $(i+1)$th points on the same rigid body for small motion by

$$w_{i+1} = w_i + \theta_i \times r_i = w_i - R_i \theta_i \tag{7}$$

$$\theta_{i+1} = \theta_i \tag{8}$$

where

$$R_i = \begin{bmatrix} 0 & -r_z & r_y \\ r_z & 0 & -r_x \\ -r_y & r_x & 0 \end{bmatrix}_i$$

Besides, we can transform the force system from the ith point to the $(i+1)$th point to get

$$f_{i+1} = f_i \tag{9}$$

$$\tau_{i+1} = \tau_i - r_i \times f_i = \tau_i - R_i f_i \tag{10}$$

Combining Eqs. (7–10), one has

$$\begin{Bmatrix} x \\ q \end{Bmatrix}_{i+1} = \begin{bmatrix} T_1 & 0 \\ 0 & T_2 \end{bmatrix}_i \begin{Bmatrix} x \\ q \end{Bmatrix}_i \tag{11}$$

where

$$T_1 = \begin{bmatrix} I & -R \\ 0 & I \end{bmatrix}, \qquad T_2 = \begin{bmatrix} I & 0 \\ -R & I \end{bmatrix}$$

As one transforms the force system from the ith point to the $(i+1)$th point, Eq. (11) relates the generalized force vector q as well as the displacement vector x at these two points.

The beam dynamics includes the motion in elongation, torsion, and bending. First, we consider the elongational motion of a beam i with length L, cross-sectional area A, Young's modulus E, and mass density ρ. The equation of motion is

$$E_i A_i w'' = \rho_i A_i s^2 w \tag{12}$$

where s denotes the time derivative and w is the displacement of the beam in elongation, and the solution is

$$w = a_i \sin \alpha_i^e z + b_i \cos \alpha_i^e z \tag{13}$$

where $\alpha_i^e = j\sqrt{(\rho_i/E_i)}s$. At one end of the beam ($z = 0$), the displacement $w(0)$ and the normal force $f(0)$ can be expressed as

$$w_i = w(0) = b_i$$

$$f_i = f(0) = -E_i A_i w'(0) = -E_i A_i \alpha_i^e a_i$$

or

$$\begin{Bmatrix} a \\ b \end{Bmatrix}_i = \begin{bmatrix} 0 & -\dfrac{1}{EA\alpha^e} \\ 1 & 0 \end{bmatrix}_i \begin{Bmatrix} w \\ f \end{Bmatrix}_i \tag{14}$$

Similarly, at the other end of the beam ($z = L$), the corresponding quantities are

$$w_{i+1} = w(L_i) = a_i \sin\alpha_i^e L_i + b_i \cos\alpha_i^e L_i$$

$$f_{i+1} = f(L_i) = E_i A_i w'(L_i) = E_i A_i \alpha_i^e \left(a_i \cos\alpha_i^e L_i - b_i \sin\alpha_i^e L_i\right)$$

or

$$\begin{Bmatrix} w \\ f \end{Bmatrix}_{i+1} = \begin{bmatrix} \sin\alpha^e L & \cos\alpha^e L \\ EA\alpha^e \cos\alpha^e L & -EA\alpha^e \sin\alpha^e L \end{bmatrix}_i \begin{Bmatrix} a \\ b \end{Bmatrix}_i \tag{15}$$

From Eqs. (14) and (15), we obtain

$$\begin{Bmatrix} w \\ f \end{Bmatrix}_{i+1} = [FE]_i \begin{Bmatrix} w \\ f \end{Bmatrix}_i \tag{16}$$

where the transfer matrix $[FE]_i$ for the motion in elongation is

$$[FE]_i = \begin{bmatrix} \cos\alpha^e L & -\dfrac{\sin\alpha^e L}{EA\alpha^e} \\ -EA\alpha^e \sin\alpha^e L & -\cos\alpha^e L \end{bmatrix}_i = \begin{bmatrix} e_{11} & e_{12} \\ e_{21} & e_{22} \end{bmatrix}_i$$

Next, let us consider the motion of the beam in torsion. The equation of motion is

$$G_i J_{bi} \theta'' = \rho_i J_{bi} s^2 \theta \tag{17}$$

where J_b is the moment of inertia of the cross-sectional area, G the shear modulus, and θ the angular displacement due to torsion. Similarly, one can derive

$$\begin{Bmatrix} \theta \\ \tau \end{Bmatrix}_{i+1} = [FT]_i \begin{Bmatrix} \theta \\ \tau \end{Bmatrix}_i \tag{18}$$

where τ is the applied torque and the transfer matrix for the motion in torsion is

$$[FT]_i = \begin{bmatrix} \cos\alpha^t L & -\dfrac{\sin\alpha^t L}{GJ\alpha^t} \\ -GJ\alpha^t \sin\alpha^t L & -\cos\alpha^t L \end{bmatrix}_i = \begin{bmatrix} t_{11} & t_{12} \\ t_{21} & t_{22} \end{bmatrix}_i$$

with $\alpha_i^t = j\sqrt{(\rho_i / G_i)}s$.

Finally, let us consider the bending motion of the beam. The equation of motion is

$$E_i I_{bi} w'''' - \rho_i I_{bi} s^2 w'' + \rho_i A_i s^2 w = 0 \tag{19}$$

where I_b is the moment of inertia of the cross-sectional area and w is the deflection due to bending. Similarly, one can derive

$$\begin{Bmatrix} w \\ \theta \\ f \\ \tau \end{Bmatrix}_{i+1} = [FB]_i \begin{Bmatrix} w \\ \theta \\ f \\ \tau \end{Bmatrix}_i \tag{20}$$

where θ, f, and τ are the slope (i.e., w'), shear force, and bending moment, respectively, and the transfer matrix for the bending motion is

$$[FB]_i = \frac{1}{2} \begin{bmatrix} cn + ch & \dfrac{sn}{\beta_1} + \dfrac{sh}{\beta_2} & -\dfrac{sn}{h_1} + \dfrac{sh}{h_2} & -\dfrac{cn}{h_3} + \dfrac{ch}{h_4} \\ -\beta_1 sn + \beta_2 sh & cn + ch & -\dfrac{\beta_1}{h_1} cn + \dfrac{\beta_2}{h_2} ch & \dfrac{\beta_1}{h_3} sn + \dfrac{\beta_2}{h_4} sh \\ -(h_1 sn + h_2 sh) & \dfrac{h_1}{\beta_1} cn - \dfrac{h_2}{\beta_2} ch & -(cn + ch) & \dfrac{h_1}{h_3} sn - \dfrac{h_2}{h_4} sh \\ h_3 cn - h_4 ch & \dfrac{h_3}{\beta_1} sn - \dfrac{h_4}{\beta_2} sh & -\dfrac{h_3}{h_1} sn - \dfrac{h_4}{h_2} sh & -(cn + ch) \end{bmatrix}_i = \begin{bmatrix} b_{11} & b_{12} & b_{13} & b_{14} \\ b_{21} & b_{22} & b_{23} & b_{24} \\ b_{31} & b_{32} & b_{33} & b_{34} \\ b_{41} & b_{42} & b_{43} & b_{44} \end{bmatrix}_i$$

where

$$\beta_1^2 = \frac{-\rho I s^2 + s\sqrt{(\rho I s)^2 - 4\rho AEI}}{2EI}$$

$$\beta_2^2 = \frac{\rho I s^2 + s\sqrt{(\rho I s)^2 - 4\rho AEI}}{2EI}$$

$$k_1 = EI, \qquad k_2 = \rho I$$

$$h_1 = k_1\beta_1^3 + k_2\beta_1 s^2, \qquad h_2 = k_1\beta_2^3 - k_2\beta_2 s^2$$

$$h_3 = k_1\beta_1^2, \qquad h_4 = k_1\beta_2^2$$

$$sn = \sin\beta_1 L, \qquad cn = \cos\beta_1 L$$

$$sh = \sinh\beta_2 L, \qquad ch = \cosh\beta_2 L$$

It is noted that the deflection and shear force have the same sign definition of the direction but the slope and bending moment have the opposite sign definition of the direction. If the sign definition of the direction for any variable is changed, we need to modify the transfer matrix. For example, changing the sign definition of the direction for θ, we have

$$\begin{Bmatrix} w \\ -\theta \\ f \\ \tau \end{Bmatrix}_{i+1} = \begin{bmatrix} b_{11} & b_{12} & b_{13} & b_{14} \\ b_{21} & b_{22} & b_{23} & b_{24} \\ b_{31} & b_{32} & b_{33} & b_{34} \\ b_{41} & b_{42} & b_{43} & b_{44} \end{bmatrix}_i \begin{Bmatrix} w \\ -\theta \\ f \\ \tau \end{Bmatrix}_i$$

or

$$\begin{Bmatrix} w \\ \theta \\ f \\ \tau \end{Bmatrix}_{i+1} = \begin{bmatrix} b_{11} & -b_{12} & b_{13} & b_{14} \\ -b_{21} & b_{22} & -b_{23} & -b_{24} \\ b_{31} & b_{32} & b_{33} & b_{34} \\ b_{41} & b_{42} & b_{43} & b_{44} \end{bmatrix}_i \begin{Bmatrix} w \\ \theta \\ f \\ \tau \end{Bmatrix}_i \tag{21}$$

From Eqs. (16), (18), (20), and (21), one can obtain the relationship between two ends of an Euler beam:

$$\begin{Bmatrix} w_x \\ w_y \\ w_z \\ \theta_x \\ \theta_y \\ \theta_z \\ f_x \\ f_y \\ f_z \\ \tau_x \\ \tau_y \\ \tau_z \end{Bmatrix}_{i+1} = \begin{bmatrix} b_{11} & 0 & 0 & 0 & -b_{12} & 0 & b_{13} & 0 & 0 & 0 & b_{14} & 0 \\ 0 & b_{11} & 0 & b_{12} & 0 & 0 & 0 & b_{13} & 0 & -b_{14} & 0 & 0 \\ 0 & 0 & e_{11} & 0 & 0 & 0 & 0 & 0 & e_{12} & 0 & 0 & 0 \\ 0 & b_{21} & 0 & b_{22} & 0 & 0 & 0 & b_{23} & 0 & -b_{24} & 0 & 0 \\ -b_{21} & 0 & 0 & 0 & b_{22} & 0 & -b_{23} & 0 & 0 & 0 & -b_{24} & 0 \\ 0 & 0 & 0 & 0 & 0 & t_{11} & 0 & 0 & 0 & 0 & 0 & t_{12} \\ b_{31} & 0 & 0 & 0 & -b_{32} & 0 & b_{33} & 0 & 0 & 0 & b_{34} & 0 \\ 0 & b_{31} & 0 & b_{32} & 0 & 0 & 0 & b_{33} & 0 & -b_{34} & 0 & 0 \\ 0 & 0 & e_{21} & 0 & 0 & 0 & 0 & 0 & e_{22} & 0 & 0 & 0 \\ 0 & -b_{41} & 0 & -b_{42} & 0 & 0 & 0 & -b_{43} & 0 & b_{44} & 0 & 0 \\ b_{41} & 0 & 0 & 0 & -b_{42} & 0 & b_{43} & 0 & 0 & 0 & b_{44} & 0 \\ 0 & 0 & 0 & 0 & 0 & t_{21} & 0 & 0 & 0 & 0 & 0 & t_{22} \end{bmatrix}_i \begin{Bmatrix} w_x \\ w_y \\ w_z \\ \theta_x \\ \theta_y \\ \theta_z \\ f_x \\ f_y \\ f_z \\ \tau_x \\ \tau_y \\ \tau_z \end{Bmatrix}_i$$

or in short

$$\begin{Bmatrix} x \\ q \end{Bmatrix}_{i+1} = \begin{bmatrix} F_1 & F_2 \\ F_3 & F_4 \end{bmatrix}_i \begin{Bmatrix} x \\ q \end{Bmatrix}_i \tag{22}$$

Now, as shown in Fig. 1, we define the shuttle end of the mast as point 1, the reflector end of the mast as point 2, and the center of mass of the reflector as point 3 or 4. The relationship between points 1 and 2 can be obtained from the beam dynamics (22):

$$\begin{Bmatrix} x \\ q \end{Bmatrix}_2 = \begin{bmatrix} F_1 & F_2 \\ F_3 & F_4 \end{bmatrix}_1 \begin{Bmatrix} x \\ q \end{Bmatrix}_1 \tag{23}$$

Transforming the force system from points 2 to 3, as shown in Eq. (11), yields

$$\begin{Bmatrix} x \\ q \end{Bmatrix}_3 = \begin{bmatrix} T_1 & 0 \\ 0 & T_2 \end{bmatrix}_2 \begin{Bmatrix} x \\ q \end{Bmatrix}_2 \tag{24}$$

The rigid-body dynamics (6) gives the relationship between points 3 and 4:

$$\begin{Bmatrix} x \\ q \end{Bmatrix}_4 = \begin{bmatrix} I & 0 \\ s^2\bar{M} + \bar{G} & I \end{bmatrix}_3 \begin{Bmatrix} x \\ q \end{Bmatrix}_3 \tag{25}$$

From Eqs. (23–25), one can obtain the relationship between points 1 and 4:

$$\begin{Bmatrix} x \\ q \end{Bmatrix}_4 = \begin{bmatrix} I & 0 \\ s^2\bar{M} + \bar{G} & I \end{bmatrix}_3 \begin{bmatrix} T_1 & 0 \\ 0 & T_2 \end{bmatrix}_2 \begin{bmatrix} F_1 & F_2 \\ F_3 & T_4 \end{bmatrix}_1 \begin{Bmatrix} x \\ q \end{Bmatrix}_1 \tag{26}$$

Because point 1 is clamped, $\{x\}_1 = 0$, one can obtain

$$\{x\}_4 = [T_1]_2[F_2]_1\{q\}_1 \tag{27}$$

$$\{q\}_4 = ((s^2[\bar{M}]_3 + [\bar{G}]_3)[T_1]_2[F_2]_1 + [T_2]_2[F_4]_1)\{q\}_1 \tag{28}$$

Recall that the displacement vector $\{x\}_4$ and the generalized force $\{q\}_4$ are applied at the center of mass of the reflector. Let $x = \{x\}_4$ and $q = \{q\}_4$. After eliminating $\{q\}_1$ from Eqs. (27) and (28), one can derive

$$M_r s^2 x + A(s)x = q \tag{29}$$

where $M_r = [\bar{M}]_3$, $A(s) = [\bar{G}]_3 + [T_2]_2[F_4]_1([T_1]_2[F_2]_1)^{-1}$. Because three reaction wheels and one collocated three-axis rate gyroscope are used to provide the control input u and the measurement v, respectively, the system becomes

$$M_r s^2 x + A(s)x = Bu \tag{30}$$

$$v = B^T s x \tag{31}$$

where

$$B = \begin{bmatrix} 0_{3\times 3} \\ I_{3\times 3} \end{bmatrix}, \qquad u = \{\tau_x \quad \tau_y \quad \tau_z\}^T, \qquad v = \{\dot{\theta}_x \quad \dot{\theta}_y \quad \dot{\theta}_z\}^T$$

It is noted that M_r is constant and the matrix $A(s)$ contains sinusoidal functions and hyperbolic functions of s. One may design a controller based on this distributed-parameter model.[4] However, in this paper, we will start to design an optimal controller by using a reduced finite-dimensional model. The distributed-parameter model is derived for the purpose of parameter estimation.

Now let us take the first two terms of Taylor's series expansion of $A(s)$ to obtain a reduced-order model:

$$M\ddot{x} + Kx = Bu \tag{32}$$

$$v = B^T \dot{x} \tag{33}$$

where $M = M_r + (1/2)A''(0)$, $K = A(0)$. This model can also be derived from the finite element method.

Modal-Space Model

In this section, the finite-dimensional model is transformed into a modal space so that all the modes are internally decoupled. The modal frequency ω_k and the mode shape e_k for the kth mode can be obtained by solving an eigenvalue problem where the mode shapes are orthonormalized with mass matrix M. Thus, one can have

$$M\omega_k^2 e_k = Ke_k, \qquad e_j^T M e_k = \delta_{jk} \tag{34}$$

where δ is the Kronecker delta. We can choose any N modes, not necessarily the first N modes, for further approximation. Substitute $x = \sum_1^N e_k y_k$ into Eq. (32) to get

$$\sum_1^N Me_k\ddot{y}_k + Ke_k y_k = Bu \tag{35}$$

Multiplying e_j^T on both sides, one obtains

$$\sum_1^N e_j^T Me_k\ddot{y}_k + e_j^T Ke_k y_k = e_j^T Bu \qquad j = 1, 2, \ldots, N \tag{36}$$

Applying Eq. (34) to Eq. (36) yields

$$\ddot{y}_j + \omega_j^2 y_j = e_j^T Bu \qquad j = 1, 2, \ldots, N \tag{37}$$

or in matrix form

$$\ddot{y} + \Lambda_N y = B_N u \tag{38}$$

where

$$y = \{y_1, \ldots, y_N\}^T, \qquad \Lambda_N = \operatorname{diag}\left[\omega_1^2, \ldots, \omega_N^2\right]$$

$$B_N = \begin{bmatrix} e_1^T B \\ \vdots \\ e_N^T B \end{bmatrix}$$

Similarly, the output equation (33) becomes

$$v = \sum_{1}^{N} B^T e_k \dot{y}_k = B_n^T \dot{y} \tag{39}$$

Equations (38) and (39) are the modal-space model derived for the control design presented in the next section.

LQG Controller Design

In this section, we propose an LQG controller based on the modal-space model and derive the explicit solutions for the corresponding Riccati equations of the optimal estimator and controller. We start by transforming the dynamic model from the modal space to a state space. Let

$$\begin{aligned}\xi &= \{\xi_1 \quad \xi_2 \quad \cdots \quad \xi_{2N-1} \quad \xi_{2N}\}^T \\ &= \{y_1 \quad \dot{y}_1/\omega_1 \quad \cdots \quad y_N \quad \dot{y}_N/\omega_N\}^T\end{aligned} \tag{40}$$

and the model becomes

$$\dot{\xi} = \mathcal{A}\xi + \mathcal{B}u + \delta \tag{41}$$

$$v = C\xi + \eta \tag{42}$$

where

$$\mathcal{A} = \text{diag}\left[\begin{bmatrix} 0 & \omega_1 \\ -\omega_1 & 0 \end{bmatrix} \quad \cdots \quad \begin{bmatrix} 0 & \omega_N \\ -\omega_N & 0 \end{bmatrix}\right]$$

$$\mathcal{B} = \begin{bmatrix} 0 \\ e_1^T B/\omega_1 \\ \vdots \\ 0 \\ e_N^T B/\omega_N \end{bmatrix}$$

$$C = \begin{bmatrix} 0 & B^T e_1 \omega_1 & \cdots & 0 & B^T e_N \omega_N \end{bmatrix}$$

Here we assume that the transformed state-space model is subjected to additive process noise δ and measurement noise η. Both are assumed to be Gaussian, zero mean, and white with constant covariance matrices N_δ and N_η, respectively. They are also assumed to be statistically uncorrelated with each other. Since the system dynamics and the measurements are corrupted by noises, this problem becomes an LQG problem, and we start to solve it with an optimal estimator design.

For the linear time-invariant dynamic system (41) and (42), the optimal state estimator is[11]

$$\dot{\hat{\xi}} = \mathcal{A}\hat{\xi} + \mathcal{B}u + LC^T N_\eta^{-1}(v - C\hat{\xi}) \tag{43}$$

where $\hat{\xi}$ is the estimate of the state ξ and the matrix L has to satisfy the Riccati equation

$$\mathcal{A}L + L\mathcal{A}^T + N_\delta - LC^T N_\eta^{-1} CL = 0 \tag{44}$$

Next, we want to find the closed-form solution of this Riccati equation by choosing $N_\eta = d_\eta I$, $N_\delta = S\mathcal{B}\mathcal{B}^T S^T$, where $S = \text{diag}[s_1 \; s_1 \cdots s_N \; s_N]$. From the process noise covariance N_δ, it can be seen that the effect of the process noise to the ith mode can be adjusted by choosing a suitable parameter s_i directly. It is expected that s_i also affects the estimator gain for the ith mode. Let us try a diagonal L and denote

$$L = \text{diag}[l_1 \quad l_1 \quad \cdots \quad l_N \quad l_N] \tag{45}$$

We can easily prove that

$$\mathcal{A}L + L\mathcal{A}^T = 0 \tag{46}$$

$$N_\delta = \begin{bmatrix} 0 & 0 & \cdots & 0 & 0 \\ 0 & e_1^T BB^T e_1 s_1^2/\omega_1^2 & \cdots & 0 & e_1^T BB^T e_N s_1 s_N/\omega_1\omega_N \\ \vdots & \vdots & \ddots & \vdots & \vdots \\ 0 & 0 & \cdots & 0 & 0 \\ 0 & e_1^T BB^T e_N s_1 s_N/\omega_1\omega_N & \cdots & 0 & e_N^T BB^T e_N s_N^2/\omega_N^2 \end{bmatrix} \tag{47}$$

$$LC^T N_\eta^{-1} CL = \frac{1}{d_\eta} \times \begin{bmatrix} 0 & 0 & \cdots & 0 & 0 \\ 0 & e_1^T BB^T e_1 l_1^2 \omega_1^2 & \cdots & 0 & e_1^T BB^T e_N l_1 l_N \omega_1 \omega_N \\ \vdots & \vdots & \ddots & \vdots & \vdots \\ 0 & 0 & \cdots & 0 & 0 \\ 0 & e_1^T BB^T e_N l_1 l_N \omega_1 \omega_N & \cdots & 0 & e_N^T BB^T e_N l_N^2 \omega_N^2 \end{bmatrix} \tag{48}$$

Substituting Eqs. (46–48) into Eq. (44) yields

$$L = \sqrt{d_\eta}\,\text{diag}\left[s_1/\omega_1^2 \quad s_1/\omega_1^2 \quad \cdots \quad s_N/\omega_N^2 \quad s_N/\omega_N^2\right] \tag{49}$$

This is the explicit solution derived for the optimal estimator (43) and s_i weighs the sensor information used for the state estimation for the ith mode.

Next let us consider the optimal control design with a performance index,

$$\text{PI} = \frac{1}{2} E\left[\int_0^\infty (\xi^T Q\xi + u^T Ru)\,dt\right] \tag{50}$$

where $E[\cdot]$ is the expectation operator. The optimal control input is[11]

$$u = -R^{-1}\mathcal{B}^T K\hat{\xi} \tag{51}$$

and the matrix K has to satisfy the Riccati equation

$$K\mathcal{A} + \mathcal{A}^T K + Q - K\mathcal{B}^T R^{-1}\mathcal{B}K = 0 \tag{52}$$

Similarly, if we choose $Q = H^T C^T CH$ ($H = \text{diag}[h_1\, h_1 \ldots h_N\, h_N]$) and R is an identical matrix, respectively, the closed-form solution can be found as

$$K = \text{diag}\left[h_1\omega_1^2 \quad h_1\omega_1^2 \quad \cdots \quad h_N\omega_N^2 \quad h_N\omega_N^2\right] \tag{53}$$

This is the explicit solution derived for the optimal controller (51) and h_i weighs the contribution of the actuators to the ith mode. From the weighting matrix Q, it can be seen that the weighting of the ith mode performance can be adjusted by choosing a suitable parameter h_i directly.

Transforming the estimator (43) and the controller (51) back to the modal space, we have

$$\ddot{\hat{y}} + \left(UB_N B_N^T + B_N B_N^T P\right)\dot{\hat{y}} + \Lambda_N \hat{y} = UB_N v \tag{54}$$

$$u = -B_N^T P\dot{\hat{y}} \tag{55}$$

where

$$U = \sqrt{1/d_\eta}\,\text{diag}[s_1 \quad s_2 \quad \cdots \quad s_N]$$

$$P = \text{diag}[h_1 \quad h_2 \quad \cdots \quad h_N]$$

$$\hat{y} = \{\hat{y}_1 \quad \hat{y}_2 \quad \cdots \quad \hat{y}_N\}^T = \{\hat{\xi}_1 \quad \hat{\xi}_3 \quad \cdots \quad \hat{\xi}_{2N-1}\}^T$$

Table 1 Identified parameters of SCOLE configuration

Mast		Reflector
$L = 125.5$ in.	$E = 30 \times 10^6$ psi	$r = \{r_x, r_y, r_z\}^T = \{1.795, 4.319, 0.\}^T$ in.
$A = 0.108$ in.^{2}	$G = 13.3 \times 10^6$ psi	$m = 0.864$ slug
$I_b = 6.66 \times 10^{-3}$ in.^{4}	$J_b = 1.33 \times 10^{-2}$ in.^{4}	
$\rho = 0.0205$ slug/in.^{3}		$J = \begin{bmatrix} 110 & -28 & -0.7 \\ -28 & 74 & -1.6 \\ -0.7 & -1.6 & 184 \end{bmatrix}$ slug-in.^{2}

Equations (54) and (55) represent the explicit optimal LQG controller, and matrices U and P are the design parameters. It is noted that both the parameter h_i of P and the parameter s_i of U are directly related to the performance of the ith mode so that it can be easily adjusted by choosing suitable design parameters for that mode. Both design parameters also contribute damping to the controller dynamics. In addition, for N desired controlled modes, we have $2N$ design parameter (N for the optimal estimator and another N for the optimal controller). It provides an easier way for the controller design to achieve a specific performance requirement.

This optimal LQG controller can also be represented by a transfer function. After taking Laplace transformation of Eqs. (54) and (55) and eliminating the state of the estimator $\hat{y}$, we have

$$u = \Psi(s)v \tag{56}$$

with

$$\Psi(s) = -sB_N^T P\left(s^2 + \left(UB_N B_N^T + B_N B_N^T P\right)s + \Lambda_N\right)^{-1} UB_N$$

This explicit LQG optimal controller is obtained based on a finite-dimensional model in the modal space. It is interesting to see that if we choose P and U to be a scalar times an identity matrix and let N go to infinity, this controller is the same as the explicit LQG optimal controller derived based on the distributed-parameter model.[12] Finally, we can also check any closed-loop pole for the uncontrolled modes by determining the roots of the characteristic equation based on the distributed-parameter model (29),

$$\det\left[s^2 M_r + A(s) - sB\Psi(s)B^T\right] = 0 \tag{57}$$

Analytical and Experimental Results

The experimental setup basically consists of a digital controller that is sandwiched between analog-to-digital and digital-to-analog converters. Since the bandwidth of both actuators and sensors is more than 10 times higher than the highest controlled modal frequency, we ignore the dynamics of actuators and sensors. The identified parameters of the SCOLE configuration are listed in Table 1. From the experiment, it is found that the sixth modal excitation damps out within 2 s with more than 10 Hz frequency. Therefore we choose the first five modes to design the controller. The first five modal frequencies identified from the analytical model also match those from the testing data (see Table 2). Since the highest controlled modal frequency is about 4.4 Hz, a sampling rate of 50 Hz for the digital controller is sufficiently fast. From the free decay response of the experiment, it can be found that the corresponding dampings are 0.19, 0.19, 0.17, 0.30, and 1.07%, respectively. The first two modes are found to be the hardest two to control.

Before the experiment, numerical simulations are performed in order to choose suitable design parameters. Tables 3 and 4 show the different design parameters used and the corresponding damping ratios, respectively. Cases 1–6 are the results from numerical simulations and the last one (test) is from testing. Let $P = 2.5I$. It can be seen that the closed-loop damping ratios are increased as U is increased until $U = P$ (see cases 1 and 2). Since the damping ratios are not improved for $U > P$ (case 3), we decide to use $U = P$ in the experiment. However, the damping ratios of the first two modes are still low, so we increase the weighting of the first two modes by using the values shown in case 4 (see Table 3). Then the damping ratios of the first two modes are significantly increased

Table 2 Identified modal frequencies

Mode	Mode shape	Measured, Hz	Identified, Hz
1	First bending in $X'Z$	0.4512	0.4514
2	First bending in $Y'Z$	0.4567	0.4524
3	First torsion	1.5223	1.5250
4	Second bending in $X'Z$	3.1333	3.2264
5	Second bending in $Y'Z$	4.3926	4.4019

Table 3 Design parameters

Case	Matrix P	Matrix U
1	$2.5I$	I
2	$2.5I$	$2.5I$
3	$2.5I$	$5I$
4	diag [10, 10, 2.5, 2.5, 2.5]	diag[10, 10, 2.5, 2.5, 2.5]
5	diag [13, 13, 2.5, 2.6, 1.9]	diag[13, 13, 2.5, 2.6, 1.9]
6[a]	diag[13, 13, 2.5, 2.6, 1.9]	diag[13, 13, 2.5, 2.6, 1.9]
Test	diag[13, 13, 2.5, 2.6, 1.9]	diag[13, 13, 2.5, 2.6, 1.9]

[a]Assume that each modal frequency has 2% error.

Table 4 Comparison of damping ratios, %

Mode	Case 1	Case 2	Case 3	Case 4	Case 5	Case 6	Test
1	0.38	0.96	0.96	3.85	5.01	2.89	2.27
2	0.38	0.95	0.95	3.84	4.95	2.84	2.20
3	4.06	10.14	10.14	10.14	10.14	7.05	2.45
4	1.93	4.82	4.82	4.82	5.01	2.78	2.13
5	2.67	6.66	6.66	6.66	5.06	2.83	2.15

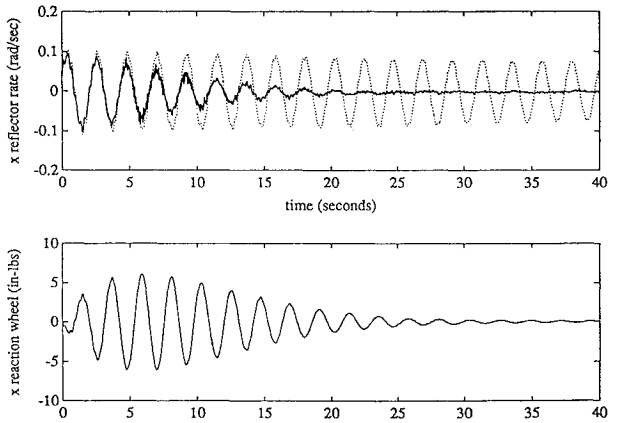

Fig. 2 Experimental result of mode 1 excitation.

(see Table 4). After considering the torque limitation for the actuator (6.3 in.-lb) and the satisfactory damping ratios, we decide to use $P = U = \text{diag}[13, 13, 2.5, 2.6, 1.9]$ for the remaining cases.

In the experiment, each mode is individually excited for 40 s and then the explicit LQG controller is activated. This procedure is repeated for all the five modes with the same controller. Figures 2–6 show the time responses [with control (solid line) and without control (dotted line)] and the corresponding control input for modes 1–5, respectively. In each figure, only the results of the dominant

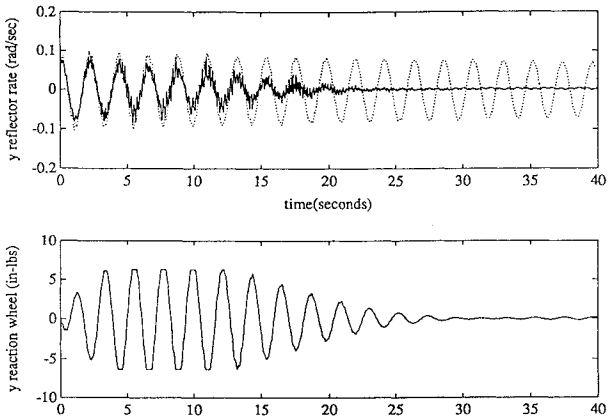

Fig. 3 Experimental result of mode 2 excitation.

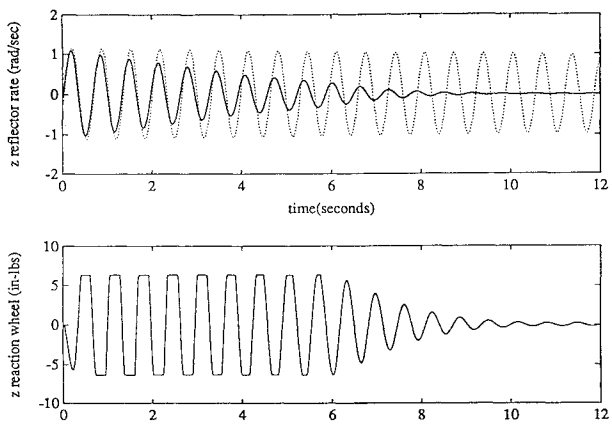

Fig. 4 Experimental result of mode 3 excitation.

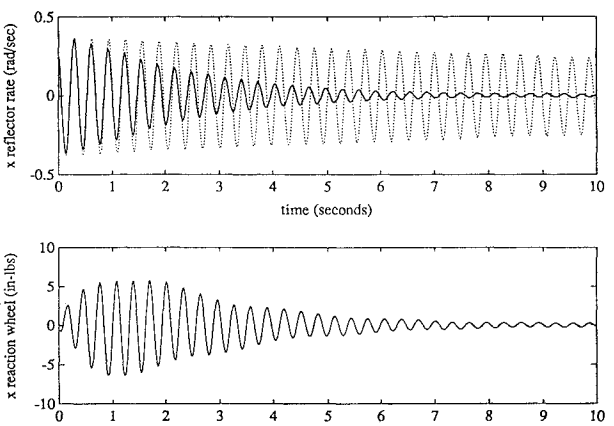

Fig. 5 Experimental result of mode 4 excitation.

axis are plotted. The results demonstrate that the controller provides sufficient damping, which means approximately 80% of amplitude decay in 10 s, for all the controlled modes. However, the damping radios (see Table 4, last column) are less than those predicted in case 5. This may be caused by the modeling error in the controller design. Let us assume that the modal frequencies used in the controller design are 2% higher than those of the actual system. The result shows that the damping ratios from the simulation (case 6) are very close to those of the experiment except the third mode. The reason may be attributed to the control input, which saturates at the torque limitation for most of the time (see Fig. 4, z reaction wheel). Although the performance of the system through the optimal controller design is very sensitive to the modeling error, the dampings still can be significantly improved. In summary, both analytical and experimental results show that the proposed explicit LQG controller not only enhances the structural damping effectively but also provides an easy way to choose the design parameters correspondingly.

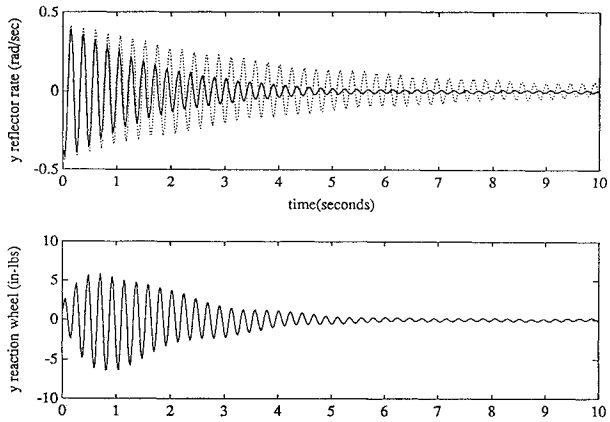

Fig. 6 Experimental result of mode 5 excitation.

Concluding Remarks

In the optimal LQG control design, one usually faces the problem of choosing suitable weighting matrices and noise covariances. It is also quite time consuming to solve the corresponding Riccati equations, particularly for large-scale systems. To overcome these problems, this paper presents an explicit optimal LQG controller (i.e., closed-form solutions to Riccati equations) for a finite-dimensional model in modal space. The number of design parameters (i.e., elements of weighting matrices and noise covariances) is also reduced and can be easily selected to achieve the desired damping for each mode. On the other hand, a simple and systematic procedure for obtaining distributed-parameter models through the transfer matrix method is also presented. The transfer matrix method and the explicit optimal LQG controller design are applied to NASA's SCOLE configuration. Both analytical and experimental results demonstrate that this proposed controller is easy to design and implement. It can also suppress vibrations effectively for large flexible structures.

Acknowledgment

This work was sponsored by NASA Langley Research Center under task order NAS1-18584-142.

References

[1]Gibson, J. S., and Adamian, A., "Approximation Theory for Linear-Quadratic-Gaussian Optimal Control of Flexible Structures," *SIAM Journal of Control and Optimization*, Vol. 29, No. 1, 1991, pp. 1–37.

[2]Joshi, S. M., and Maghami, P. G., "Robust Dissipative Compensators for Flexible Spacecraft Control," *IEEE Transactions of Aerospace and Electronic Systems*, Vol. 28, No. 3, 1992, pp. 769–774.

[3]Juang, J. N., and Phan, M., "Robust Controller Designs for Second-Order Dynamic Systems: A Virtual Passive Approach," NASA TM-102666, May 1990.

[4]Balakrishnan, A. V., "Compensator Design for Stability Enhancement with Collocated Controllers," *IEEE Transactions on Automatic Control*, Vol. 36, No. 9, 1991, pp. 994–1007.

[5]Shen, J. Y., Huang, J.-K., and Taylor, L. W., Jr., "Likelihood Estimation for Distributed Parameter Models of Large Beam-Like Structures," *Journal of Sound and Vibration*, Vol. 155, No. 3, 1992, pp. 467–480.

[6]Shen, J. Y., Huang, J.-K., and Taylor, L. W., Jr., "Timoshenko Beam Modeling for Parameter Estimation of NASA Mini-Mast Truss," *ASME Journal of Vibration and Acoustics*, Vol. 155, No. 1, 1993, pp. 19–24.

[7]Taylor, L. W., Jr., "PDEMOD: Computer Software for Distributed Parameter Estimation for Flexible Spacecraft Applied to NASA Mini-Mast Truss Experiment," presented at Second USAF/NASA Workshop on System Identification and Health Monitoring of Precision Space Structures, Pasadena, CA, 1990.

[8]Pestel, E. C., and Leckie, F. A., *Matrix Methods in Elastomechanics*, McGraw–Hill, New York, 1963.

[9]Horner, G. C., "The Riccati Transfer Matrix Method," Ph.D. Dissertation, Univ. of Virginia, Charlottesville, VA, May 1975.

[10]Uhrig, R., "The Transfer Matrix Method Seen as One Method of Structural Analysis among Others," *Journal of Sound and Vibration*, Vol. 4, No. 2, 1966, pp. 136–148.

[11]Kwakernaak, H., and Sivan, R., *Linear Optimal Control Systems*, Wiley, New York, 1972.

[12]Balakrishnan, A. V., "An Explicit Solution to the Optimal LQG Problem for Flexible Structures with Collocated Rate Sensors," *Proceedings of the Fifth NASA/DOD CSI Technology Conference* (Lake Tahoe, NV), 1992.